INTERNATIONAL JOURNAL FOR NUMERICAL METHODS IN FLUIDS
Int. J. Numer. Meth. Fluids 2003; **42**:1–21 (DOI: 10.1002/fld.401)

Finite volume/mixed finite element analysis of pollutant transport and bioremediation in heterogeneous saturated aquifers

Claudio Gallo[1,2] and Gianmarco Manzini[3,*,†]

[1]*CRS4, Zona Industriale Macchiareddu, Uta, Cagliari, Italy*
[2]*Department of Civil Engineering and Geosciences, TUDelft, Delft, The Netherlands*
[3]*IAN-CNR, via Ferrata 1, 27100 Pavia, Italy*

SUMMARY

The adoption of a suitable pumping–injecting well network and the human enhancement of the activity of soil bacteria, whose metabolism contributes to degrade and transform many pollutants in non-toxic substances, may be crucial in the process of remediation of contaminated soils. Organic contaminant transport in a subsurface aquifer and its biological degradation kinetics is numerically addressed by using a four contaminant species model. A numerical approach is proposed, that is based on a cell-centre finite volume method for the system of advection–dispersion equations of contaminants with a mixed-hybrid finite element method for the solution of a single-phase Darcy's equation. The effectiveness of the method and its accuracy in retaining the main physical properties of the continuous mathematical model is illustrated by simulating the time evolution of contaminant concentrations in a set of realistic scenarios. Copyright © 2003 John Wiley & Sons, Ltd.

KEY WORDS: bioremediation; contaminant transport; mixed finite elements; finite volumes

1. INTRODUCTION

Soil contamination has recently become a problem of major social concern, because a wide range of pollutant agents of different chemical nature and toxicity have been found in subsurface aquifers. Pollution sources are either accidental events, like spills and leaks, or common human activities, like disposal of urban sewage, industrial wastes, and the use of pesticides and fertilizers in agriculture, see References [1–6]. The contaminants in a subsurface aquifer are subject to complex physical and chemical processes, such as dispersion, advection by groundwater flow, chemical reactions and biological degradation due to soil microorganisms.

The groundwater flow is described by a single-phase Darcy's equation, while the subsurface transport of different chemical species are modelled by a set of coupled advection–dispersion–reaction equations [7].

* Correspondence to: G. Manzini, IAN-CNR, via Ferrata 1, 27100 Pavia, Italy.
† E-mail: marco@ian.pv.chr.it

Received June 2001
Revised 31 May 2002

The biological degradation depends on the microorganism population whose metabolism is affected by the availability in soils of substrates like organic carbon, electron acceptors—oxygen and nitrogen—and nutrients [8, 9]. The organic carbon needed to sustain bacterial life is generally present in soil as well as other nutrients—such as phosphates, nitrates, ammonia—which also contribute to microbial survival. In many cases, however, human activities may provide an additional supply both of organic carbon and of nutrients. Organic carbon is furnished in the form of accidental spills of organic contaminants, such as benzene and its derivatives or more hazardous compounds. Industrial fertilizers and manure used in agricultural activities, on the other hand, are examples of possible external supplies of nutrients. The bacterial population is normally stable because it dynamically tends to an equilibrium state in which its growth rate is balanced by its decay rate. When the concentration of the species which take part in microbial metabolism are subject to a significant increase due, for example, to an external supply, the bacterial population increases of several orders of magnitude and tends to a new equilibrium state. The remarkable fact is that the bacterial metabolic processes effectively use hazardous organic pollutants and reduce them to harmless byproducts, such as CO_2 and H_2O [10]. In this context, a remediation strategy can be devised which relies on the enhancement of the biodegradation activity, see Reference [11] for a literature review on this topic. The biodegradation kinetics models proposed in the literature are usually classified in three distinct classes, respectively, termed *free-bacteria*, *microcolony-based* and *biofilm* models [12, 13].

The simplest models belong to the first class [14]. They basically assume that bacteria exist as *individual particles* within the aqueous phase or adsorbed by soil grains. No assumption is made on the microscopic configuration and distribution of bacteria in soil pores, and on the way the organisms are grouped together on the solid pore surface. These latter facts are considered irrelevant for the macroscopic description of bacterial population growth and decay. In the second class of models, bacteria do not exist as individual particles but in small discrete colonies, or *microcolonies*, attached to the surface of soil grains. Growth and decay of the biomass contained in microcolonies are formulated either by taking that the bacterial colony dimension can grow by consumption of organic substrate and electron acceptors or by assuming the colony dimension constant and varying their *concentration*, i.e. the number of colonies per unit volume [15]. The main feature of the models in the third class is that the solid particles constituting the aquifer material are covered by a *biofilm* within which consumption of the substrates and electron-acceptors takes place [12, 13, 16]. The key processes are the mass exchange between bulk flow and the biofilm and the internal degradation of organic substrates. A more detailed discussion of the similarities and differences between these models is beyond the scope of the present work. We refer the interested reader to the discussion in Reference [17]—see also the bibliography therein—where it is shown that under a set of simplifying assumptions the three approaches reduce to an essentially equivalent description of the biodegradation process. This, however, is true only for very simple cases.

Our approach relies on the four-species model documented in References [15, 18] in the context of the more general microcolony-based concept. The main feature of this model lies in its capability of describing how the metabolism of subsurface microbes can be enhanced by concurrent metabolization of oxygen, nitrogen and nutrients. From the computational viewpoint, it is a compromise between the simpler free-bacteria model which tends to over-estimate the degradation extent, and the more accurate but also more complex and expensive bio-film model.

The numerical approximation of the complete mathematical model is a research issue, and many different aspects make the numerical simulation of a bioremediation process challenging. The most significant topics that have been investigated in the present work are listed.

- *Treatment of highly heterogeneous soil*: the value of the permeability can differ for four orders of magnitude or more between two adjacent mesh cells.
- *Advection-dominated transport*: the model species concentrations in the groundwater bulk-flow can feature strong gradient regions when sharp concentrations fronts move throughout the computational domain.
- *Non-linear coupling effects*: even if the soil is saturated, the growth/decay rate of the bacterial population depends on the contaminants which diffuse within the microcolonies from the groundwater bulk flow. It also exerts its influence on the bulk-flow contaminant concentrations via a set of reactive source terms in the transport equations.

These issues have already been investigated by the authors in these previous works. In Reference [13] we presented some preliminary results on the discretization of the flow and transport equations by using *mixed finite elements* and *finite volumes*. The coupling of the contaminant transport equations with a bacterial population equation and its numerical discretization was investigated in Reference [20]. In this work the model species are passively advected by a constant velocity and pressure fields. In order to solve the Darcy's equation we adopted a high-order accurate mixed finite element scheme ($\mathscr{BDM}_1$). Despite its accuracy, this approach is not appropriate to simulate non-linear phenomena requiring a frequent update of the velocity and pressure fields because of the high computational cost. A better approach from this viewpoint is based on the *mixed-hybrid* scheme proposed in Reference [21]. In this work we validated the method on the standard quarter-of-five-spots problem, focusing the attention on the treatment of the soil heterogeneity.

The work presented in the current paper copes with the bioremediation of a field-size aquifer that has been contaminated by an accidental leak out. Different bioremediation techniques and human intervention strategies are numerically investigated to predict the clean-up time for an almost complete removal of pollutants.

According with our previous experience we consider the following numerical approach. The steady groundwater bulk flow is approximated by using the lowest-order mixed-hybrid finite element method. This approach yields an approximation to the steady velocity field that is more accurate than those provided by straightforward differentiation of the conforming finite element approximation of the pressure field. In particular, we emphasize that the mixed-hybrid finite element method ensure local—i.e. cell-wise—mass conservation, while the conforming finite element approximation lacks local mass conservation. The contaminant transport equations are approximated in space by an unstructured triangle-based finite volume method and advanced in time by a semi-implicit two-stage Runge–Kutta scheme. A TVD stability condition is imposed by a multidimensional limiting procedure. The resulting scheme is formally second-order accurate, conservative, and capable of capturing strong solution gradient fronts moving at the correct physical propagation speeds.

The species interactions are taken into account in the full-species model by solving iteratively their non-linear interaction coupling.

The outline of the paper follows. In Section 2, we review the mathematical model describing single-phase bulk flow, contaminant transport and bacterial kinetics. The discretization

method is summarized in Section 3. We address here the finite volume discretization of the contaminant transport equations as well as the mixed-hybrid finite element approximation of the Darcy's phase pressure and velocity fields. The numerical schemes are presented in details in Reference [22]. In Section 4 we present the results of a set of numerical investigations that assess the performance of possible remediation strategies. We consider also different networks of extraction/injection wells, whose running mode has been selected on the basis of the plume location and the soil remediation status. The conclusions follow in Section 5.

2. THE MATHEMATICAL MODEL

All the partial differential equations presented in the following sub-sections are formulated in Ω, which is a two-dimensional polygonal domain with boundary $\partial\Omega$.

2.1. Transport equations

Transport phenomena are mathematically described by a system of N_{DS} coupled advection–dispersion–reaction equations, where N_{DS} is the number of dissolved species. In divergence form they can be written as follows:

$$R_i \frac{\partial C_i}{\partial t} + \mathrm{div}(\mathbf{u}C_i - \mathbf{D}_i(\mathbf{u})\nabla C_i) = B_i, \quad i = 1, \ldots, N_{\mathrm{DS}} \tag{1}$$

The variables C_i in Equation (1) represent the bulk flow concentration of each transported species; the terms R_i are the retardation factors, which take into account chemical adsorption processes, the terms $\mathbf{D}_i(\mathbf{u})$ are the dispersion tensors, which depend on the groundwater velocity field $\mathbf{u}$. The r.h.s. source terms B_i describe the coupling between the species concentrations transported in the bulk flow and the ones within microcolonies. The model adopted for these terms is presented in Section 2.3.

Equation (1) is supplemented by a set of appropriate boundary conditions, such as inlet, outlet and no-flow, and initial solution states to specify the application problems.

2.2. The Darcy's equation

Groundwater bulk flow in an heterogeneous saturated soil is mathematically formulated by the Darcy's equation [23]

$$\begin{aligned} \mathbf{u} &= -\mathbf{K}\nabla p \\ \mathrm{div}\,\mathbf{u} &= f \end{aligned} \tag{2}$$

The pressure field is indicated by p and the groundwater velocity field by $\mathbf{u}$, $\mathbf{K}(\mathbf{x})$ is the transmissivity tensor, and $f(\mathbf{x})$ a source/sink term. Equations (2) are completed by a set of suitable boundary conditions of Neumann/Dirichlet-type, modelizing inlet/outlet and no-flow boundary configurations.

2.3. The bioremediation model

Microcolony-based models assume that bacteria reside and act within microcolonies, described as a set of patches attached to soil grains [15]. From the bulk phase, chemical species can

reach microcolonies via diffusive mass exchange. Depending on the mass-transfer coefficient, concentrations within microcolonies govern the degradation rate kinetics and can be significantly different from those in the bulk phase.

In this class of models, the term B_i of Equation (1) is expressed in terms of a diffusive mass exchange from the bulk to the microcolony phase

$$B_i = N_c \kappa_i A_c \frac{(C_i - c_i)}{\delta}, \quad i = 1, \ldots, N_{DS} \tag{3}$$

where κ_i is the mass-exchange coefficient between bulk flow and microcolonies, A_c is the contact area of one microcolony for the mass diffusion process, δ is the thickness of the boundary layer between bulk flow and microcolonies, c_i is the concentration of the component i in the microcolonies and N_c is the number of microcolonies per unit volume.

The assumption that the biodegradation process works essentially at a steady-state regime yields the following form for the r.h.s. terms B_i in Equation (3):

$$\kappa_i A_c \frac{(C_i - c_i)}{\delta} = \mu_{0,i} m_c \sum_{k=1}^{N_{EA}} Y_{i,k} \left[\prod_{j=1}^{N_{DS}^i} \frac{c_j}{K_{j,k} + c_j} \right] I_b^{k-1} + Q_i I_b^{i-1}, \quad i = 1, \ldots, N_{DS} \tag{4}$$

where $\mu_{0,i}$ are the maximum rate coefficients, m_c is the mass of a microcolony, $Y_{i,k}$ are the yield coefficients which account for the stoichiometry and efficiency of degradation, $K_{j,k}$ are the half-saturation constants, and I_b^{k-1} are the inhibition functions [15]. In Equation (4) the symbol N_{EA} denotes the number of electron acceptors and N_{DS}^i the number of dissolved species involved in the degradation of the ith species. The term Q_i is non-zero only when the component i is an electron acceptor—for instance oxygen or nitrate. In this case, it takes the form

$$Q_i = \alpha_i \frac{c_i}{K_i + c_i}, \quad i = 1, \ldots, N_{EA} \tag{5}$$

where α_i is the electron acceptor coefficient for the maintenance energy of bacteria, and K_i is the electron acceptor saturation constant.

This degradation equation states that the total amount of a compound entering a microcolony in a given interval of time is equal to the amount of species that is degraded in the same interval. The rate of degradation and, consequently, the concentration within microcolonies, is roughly proportional to the concentration outside the colonies. The terms Q_i introduce into the model the consumption of oxygen due to bacterial decomposition [15, 18] as a first-order decay term.

Bacterial kinetics is modelled by the following time-dependent differential equation that describes the microcolony population dynamics

$$\frac{1}{N_c} \frac{\partial(\phi N_c)}{\partial t} = \sum_{i=1}^{N_{DH}} \left[\mu_{0,i} \sum_{k=1}^{N_{EA}} Y_{i,k} \left(\prod_{j=1}^{N_{DS}^i} \frac{c_j}{K_{j,k} + c_j} \right) \right] - k_d^c, \tag{6}$$

where k_d^c is the population decay constant, N_{DH} is the number of dissolved hydrocarbons—organic substrates—and ϕ is the porosity of the medium [15, 18].

3. THE NUMERICAL MODEL

3.1. The finite volume discretization of the transport equations

The numerical discretization in the framework of the finite volume scheme is defined on the same mesh $\mathscr{T}_h(\Omega)$ used for the mixed-hybrid scheme of the previous section. The index h is the maximum diameter of the N_T triangles forming the mesh, i.e. $h = \max_{T\in\mathscr{T}_h(\Omega)} h_T$, where h_T is the length of the longest edge of the triangle T. As usual, these triangulations are assumed *regular* and *conforming* for $h \to 0$ in the sense specified in Reference [24, p. 132].

Equation (1) is reformulated in a cell-wise integral form by integrating them on each triangular cell T and then applying the Gauss divergence theorem to transform the spatial divergence term into a balance of edge integral fluxes. Let us introduce for every $T \in \mathscr{T}_h(\Omega)$ the vector $\mathbf{U}_T$, whose elements are the cell-averaged concentrations of the transported species

$$\mathbf{U}_T|_i = \frac{1}{|T|}\int_T C_i \,\mathrm{d}T, \quad i = 1,\ldots,N_{\mathrm{DS}} \tag{7}$$

The semi-discrete finite volume approximation is

$$|T|\mathbf{R}\frac{\mathrm{d}\mathbf{U}_T}{\mathrm{d}t} + \sum_{e\in\sigma(T)} \mathbf{G}_e(\mathbf{u}_e, \tilde{\mathbf{U}}_T, \tilde{\mathbf{U}}_{T_e}, \mathbf{n}_e) + \sum_{e\in\sigma(T)} \mathbf{H}_e(\mathbf{u}_e, \tilde{\mathbf{U}}_T, \tilde{\mathbf{U}}_{T_e}, \mathbf{n}_e) + \sum_{e\in\sigma'(T)} \mathbf{F}_e^{(bc)} = \sum_q \omega_{T,q}\mathbf{S}_T(\tilde{\mathbf{U}}_T(\mathbf{x}_{T,q})) \quad \text{for every } T \in \mathscr{T}_h(\Omega) \tag{8}$$

where the diagonal matrix $\mathbf{R} = \mathrm{diag}(R_1,\ldots,R_{N_{\mathrm{DS}}})$ collects the retardation factors, and for every cell T,

- $|T|$ is the measure of its area, and ∂T its boundary,
- $\sigma(T)$ is the subset of its *internal* edges; these latters are the edges that T shares with an adjacent mesh cell indicated by T_e, so that for every $e \in \sigma(T)$ there exists a cell $T_e \in \mathscr{T}_h(\Omega)$ such that $e = \partial T \cap \partial T_e$,
- $\sigma'(T)$ is the subset of the edges of T located at the boundary of the computational domain; that is, for every $e \in \sigma'(T)$ we have $e = \partial T \cap \partial\Omega$.

The cell interface flux integral is evaluated by using suitable advective and dispersive *numerical* fluxes across the edge e, that are

$$\mathbf{G}_e(\mathbf{u}_e, \tilde{\mathbf{U}}_T, \tilde{\mathbf{U}}_{T_e}, \mathbf{n}_e)|_i \approx \int_e \mathbf{n}\cdot\mathbf{u}\mathbf{U}|_i \,\mathrm{d}l \tag{9}$$

$$\mathbf{H}_e(\mathbf{u}_e, \tilde{\mathbf{U}}_T, \tilde{\mathbf{U}}_{T_e}, \mathbf{n}_e)|_i \approx \int_e \mathbf{n}\cdot\mathbf{D}|_i(\mathbf{u})\nabla\mathbf{U}|_i \,\mathrm{d}l \tag{10}$$

and the numerical flux function $\mathbf{F}_e^{(bc)}$ at boundary edges.

The numerical flux vector functions $\mathbf{G}_e$ and $\mathbf{H}_e$ introduced in Equations (9) and (10) depend on $\mathbf{u}_e$, which is the value of the velocity field $\mathbf{u}$ at the midpoint of the edge e shared by the

triangles T and T_e, and on $\mathbf{n}_e$, which is the normal to e oriented outward from T and inward into T_e. They also depend on $\tilde{\mathbf{U}}_T$ and $\tilde{\mathbf{U}}_{T_e}$, which are the piecewise-polynomial representations of the solution in T and T_e. This functional dependence implies the usage of pointwise values of the approximate solution at quadrature nodes on e. These values are reconstructed from the cell averages by an interpolation procedure at each time step and a multidimensional slope limiter must be considered to keep under control the numerical oscillations, see the appendix of Reference [20].

The integral advective term $\mathbf{G}_e$ is discretized by a standard upwind flux splitting approach, while the integral dispersion term $\mathbf{H}_e$, which involves second-order derivatives in space, by a central differentiation algorithm. Further details about the derivation and the accuracy of this method are discussed in Reference [22].

The numerical flux function $\mathbf{F}_e^{(bc)}$ at the boundary edge $e = \partial T \cap \partial\Omega$ depends on the trace $\tilde{\mathbf{U}}_T|_e$ of the reconstructed solution $\tilde{\mathbf{U}}_T$ within the unique boundary triangle T, and in some suitable form on a set of *external* data $\mathbf{U}_e^{(bc)}$. The integral source term $\mathbf{S}_T(\tilde{\mathbf{U}}_T(\mathbf{x}_{T,q}))$ is approximated by a surface quadrature rule with nodes $\{\mathbf{x}_{T,q}\}$ within the triangle T and weights $\{\omega_{T,q}\}$.

The time-marching scheme is obtained by approximating the time derivative of $\mathbf{U}_T$—which appears in the first term in the semi-discrete formulation (8)—by first-order finite differences

$$\left.\frac{\mathrm{d}\mathbf{U}_T(t)}{\mathrm{d}t}\right|_{t=t^n} \approx \frac{\mathbf{U}_T^{n+1} - \mathbf{U}_T^n}{\Delta t} \tag{11}$$

where $\mathbf{U}_T^{n+1}$ and $\mathbf{U}_T^n$ are the cell-averaged solutions in T at times t^{n+1} and t^n, and $\Delta t = t^{n+1} - t^n$. This yields a full discrete semi-implicit scheme where resulting symmetric linear algebraic problem is solved by a standard Krylov solver, such as a preconditioned conjugate gradient method. Higher-order accuracy in time is attainable by a semi-implicit Runge–Kutta method, built by two distinct stages of the same form [22].

3.2. The mixed-hybrid discretization of the Darcy's equation

The coupled system of Equations (2) in the unknowns p and $\mathbf{u}$ is discretized by a mixed-hybrid finite element approach. For a detailed exposition of mixed and mixed-hybrid finite element methods we refer the reader to References [25, 26], while for the description of the numerical formulation adopted in this work we refer to Reference [20].

In the mixed-hybrid finite element method adopted in the present work we approximate the velocity field by using the lowest-order $\mathscr{RT}_0$ discontinuous elements, which is composed by two-dimensional functions whose restriction to any mesh triangle T is of the form

$$\mathbf{u}|_T \approx \alpha_T \begin{pmatrix} x \\ y \end{pmatrix} + \begin{pmatrix} \beta_T \\ \gamma_T \end{pmatrix} \tag{12}$$

where the real scalar coefficients α_T, β_T and γ_T depend on the triangle T. The pressure field is approximated using triangle-based piecewise constant functions while the pressure trace over each cell-interface by the edge-based piecewise constant ones.

With respect to Reference [20], the present work differs substantially in the choice of the discrete functional space used for the approximation of the velocity field $\mathbf{u}$. We use here the lowest-order $\mathscr{RT}_0$ discontinuous elements instead of the $\mathscr{BDM}_1$ ones of Reference [20], where a full linear dependence on the position is considered. Notice also that the continuity

condition of the normal component of the velocity flux is relaxed, and a weaker condition is imposed by a set of suitable Lagrange multipliers which approximates the pressure traces.

We experienced in fact that $\mathscr{R}\mathscr{T}_0$ elements offers a satisfactory accuracy level at a reduced computational cost with respect to $\mathscr{B}\mathscr{D}\mathscr{M}_1$ elements, see Reference [21]. These latter ones are formally more accurate but also significantly more demanding from a computational viewpoint because they involve twice the number of unknowns to be stored and calculated compared to $\mathscr{R}\mathscr{T}_0$. This issue is particularly important because in this work the pressure and the velocity fields are iteratively updated at each time step, see Reference [12], while in the work described in Reference [20] they were calculated only once at the beginning of each simulation and then used to transport passively the concentration fields of the contaminant species.

3.3. Reaction source terms and microbial population equation

The reaction terms described in Equation (6) are computed by solving a set of nodewise non-linear systems via a Newton iterative method with fractional multistep integration scheme [20].

4. NUMERICAL EXPERIMENTS

In this section, we illustrate the performance of the proposed mathematical and numerical model in predicting the effectiveness of a remediation intervention to reduce the contaminant concentration of a polluted aquifer. The aquifer is characterized by a constant porosity $\phi = 0.3$ and a heterogeneous isotropic transmissivity, whose principal values are assumed to be constant on each triangle of the computational mesh, and differ triangle by triangle in the range between 10^{-5} and $1\,\mathrm{m}^2/\mathrm{day}$, in accord with an equiprobability stochastic distribution.

The first test case that we present in this paper consists in the initial soil contamination phase and is labelled by $T1$. The soil contamination is due to the leakage of Cyclo-Aromatic-Hydrocarbons (CAH), which forms a plume transported by the groundwater flow field and spread in the saturated aquifer.

The next three test cases, labelled by $T2$, $T3$ and $T4$, describes three possible interventions for the remediation phase. Basically, we consider a network of pumping wells that extract the polluted water and convey it to a treatment plant, where the contaminant is removed. The purified water, which may be enriched in oxygen and nutrients to stimulate soil bacterial growth, is then re-injected in the aquifer via a network of injection wells. Figure 1 sketches the water treatment procedure.

All of the wells can be selectively used either in injection or in extraction mode and are all supposed to be connected via pipelines to the water treatment plant. The proper position and configuration of the wells have been chosen by investigating their capability of intercepting the contaminated plume transported by the groundwater flow in a set of preliminary simulations. These simulations are based on the four species model proposed by Molz *et al.* [15] and Widdowson *et al.* [18], and described in Reference [20]. For the sake of completeness, we report the model in the final appendix, giving also the values of the parameters used in the simulations. The contaminant CAH is the organic substrate S of the model, while the other species involved are the dissolved oxygen in the soil, O, some compounds chemically based on nitrates, N, and some ammonia-based compounds which constitute a generic nutrient

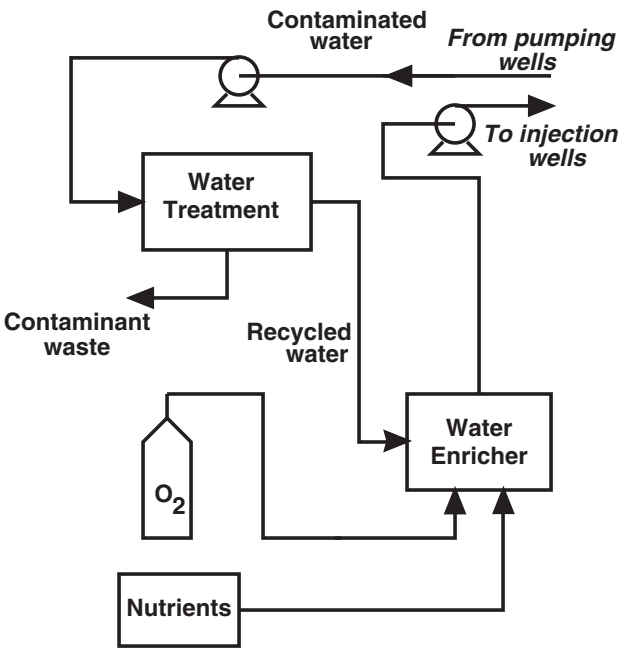

Figure 1. Technical scheme of the remediation plant installed aside of the well network for polluted water treatment and clean water enrichment.

supply A. The initial concentration of the organic substrate and the dissolved oxygen follows a random distribution, with values in the range $[0.1, 1]\,\mathrm{g/m^3}$. The initial distribution of nitrates and ammonia-based compounds takes instead a constant initial value of 1000 $\mathrm{g/m^3}$. Figure 2 depicts the benchmark case and the position of the wells on the aquifer—labels 'A'–'M'—in the remediation phase. Point 'A' is also the location of the leaking tank when contamination occurs. A constant gradient of $\Delta p/\Delta x = 0.04$ is superimposed on the subsurface flow field in the aquifer, which is thus oriented along the x direction. These model problems are completely defined by a suitable Dirichlet boundary condition, with an hydraulic pressure head given as a function of x. For each simulation run, we report in Table I the time step Δt and the final time $T_{\max}$ at which the simulation ends up. During the initial pollution phase ($T1$), the plume of CAH spreads with an irregular, or 'fingered', front because of the stochastic soil heterogeneity which establishes several preferential paths. Figure 3 illustrates the situation at the intermediate time $t = 410$ days, when the contaminant reaches the boundary of the aquifer and begins to dissolve into the water of the confining river. A steady-state solution is reached at $t = 600$ days, shown in Figure 4, when the contaminant plume does not spread further and the transport of the contaminant along some preferential paths is thus established.

In the three simulations $T2$, $T3$, and $T4$, the remediation intervention takes place after $t = 410$ days since the pollution started, that is before the contaminant reaches the river confining with the aquifer. We suppose that the contaminant source is removed and the clean-up of the soil is performed by using a network of extraction/injection wells. For all of the

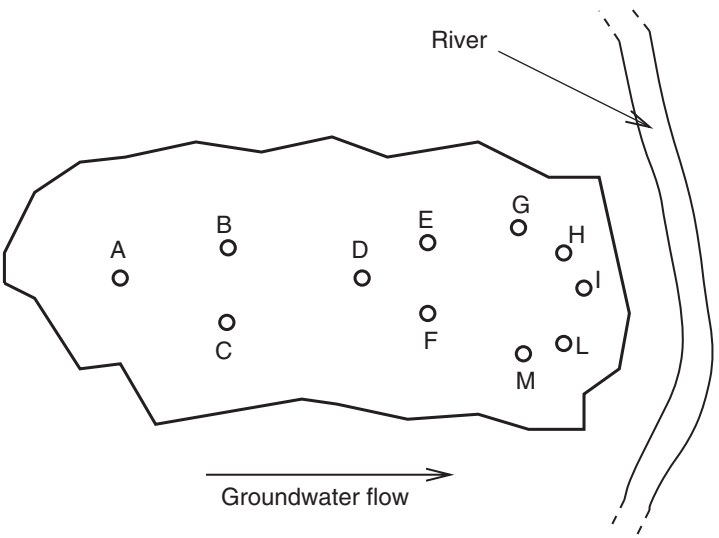

Figure 2. Planar sketch of the well locations.

Table I. Simulation run parameters.

	Run label			
Parameter	T1	T2	T3	T4
Δt (days)	0.5	0.2	0.05	0.05
T_{max} (days)	410	2800	500	700

simulations we show the spatial distribution of the organic substrate, CAH, and of the dissolved oxygen (DO)—the species O in our four species model.

In simulation $T2$ we consider the so-called *pump-and-treat* method. The wells G through M of the pipeline network are active and extract the contaminated water, which is then conveyed to water treatment plants. The flow boundary conditions are the same as for the soil contamination phase, except at the location corresponding to the pumping wells: here, a decrease of 0.5 m in pressure head with respect to the natural gradient condition is imposed in order to modify the flow pattern for contaminant recovery. As in the soil contamination phase, just one chemical species is considered in the simulation, by neglecting the effects of the other species. The results of this simulation are shown in Figure 5 at the intermediate time $t = 1450$ days, that is about 4 years after the removal of the contaminant source, and in Figure 6 at the final time of $t = 2500$ days—about 7 years. The soil heterogeneity still affects the effectiveness of the removal, but the spreading effect is not as evident as in the $T1$ phase. However, when the simulation terminates, the removal of the organic contaminant plume has not yet been fully completed.

The bioremediation interventions considered in this paper, simulations $T3$ and $T4$ are essentially based on the stimulation of the growth of the subsurface bacterial population by

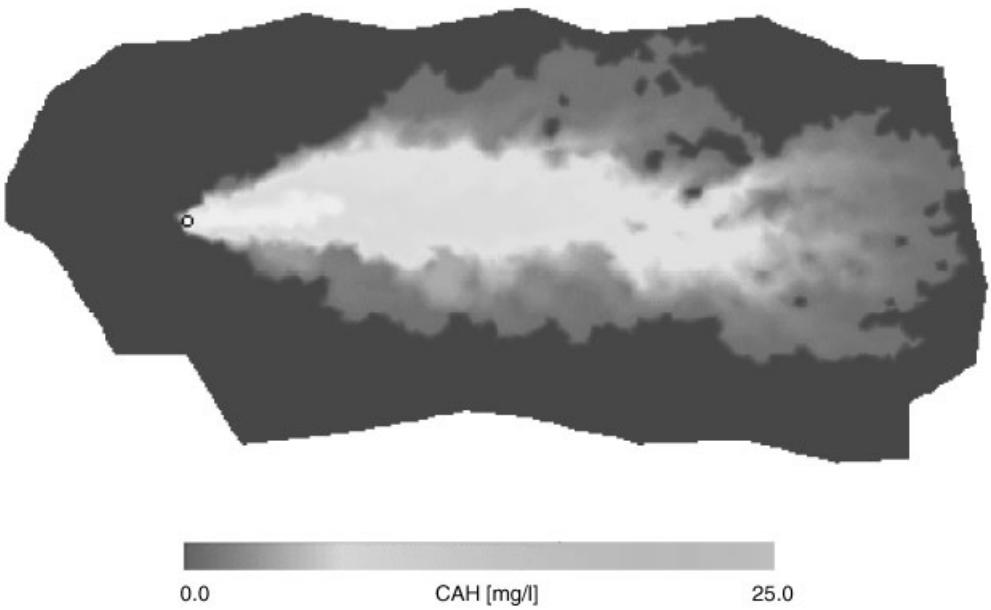

Figure 3. Contamination phase ($T1$): pollutant concentration at $t = 410$ days.

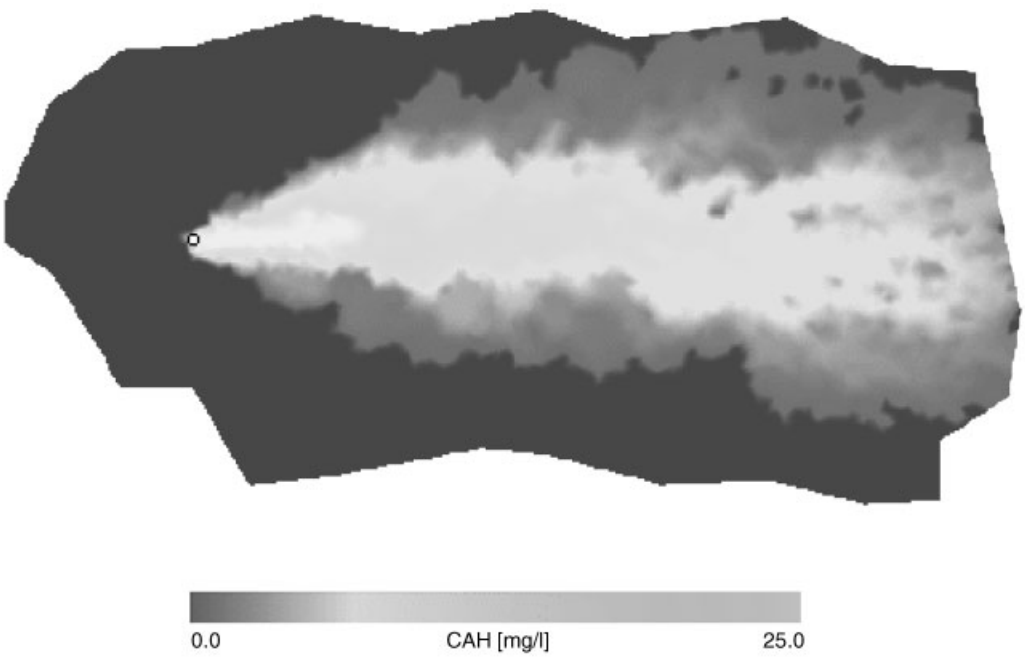

Figure 4. Contamination phase ($T1$): pollutant concentration at $t = 600$ days—steady state.

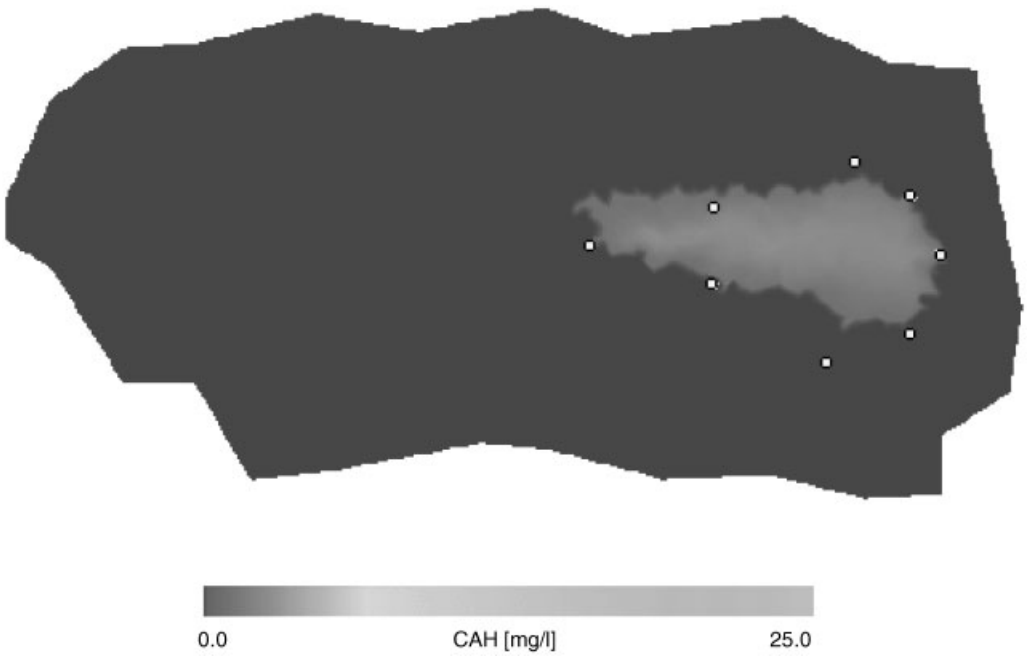

Figure 5. Pump-and-treat remediation ($T2$): concentration at $t = 1450$ days.

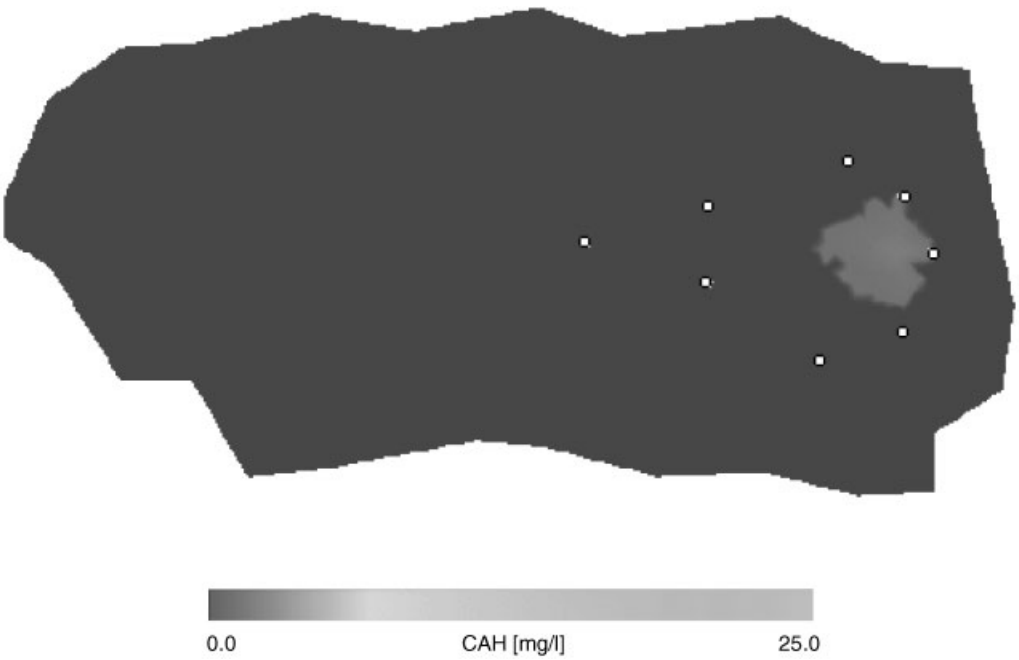

Figure 6. Pump-and-treat remediation ($T2$): concentration at $t = 2500$ days.

increasing the concentration of oxygen and nutrients dissolved in soil. We assume that these chemical substances be directly supplied via injection of 'enriched water' into the aquifer. Part of the wells are, thus, used for extracting the contaminated water to be conveyed to treatment plants. Part or all of the remaining wells are used for re-injecting water with chemical additives into the soil. The effectiveness of this strategy strongly depends on the extraction–injection operational mode chosen in the well configuration pattern, which is different for the two simulations $T3$ and $T4$.

In simulation $T3$ the wells A–D work in injection mode—an overpressure of 0.5 m is imposed. Nutrients and nitrates are delivered in excess, since their solubility in water is much larger than the one of oxygen, which is kept at a constant concentration of 20 mg/l. The remaining wells work in extraction mode, at the same pressure condition of the 'pump-and-treat' method. The results of this simulation are shown in Figure 7 at the intermediate time $t = 178$ days and in Figure 8 at the final time $t = 360$ days.

The effectiveness of this approach with respect to the 'pump-and-treat' method is clearly documented by the contaminant removal achieved in $T3$ after 1 year which is almost comparable to the one achieved in $T2$ after 7 years, see for instance Figures 8 and 6. The major difference in the contaminant distribution field is indeed in the region where dissolved oxygen has been delivered. However, the intervention simulated in $T3$ cannot be considered satisfactory because a 'dead-zone' develops in the triangular region defined by the wells 'F-G-H', all working in pumping conditions, thus preventing the complete de-contamination of the site.

A different well pattern has been experimented in simulation $T4$, wells A–D are dismissed, wells E and F inject nutrients and oxygen, and wells G–M still work in extraction mode as in $T3$. Figure 9 shows the contaminant and dissolved oxygen distributions at the intermediate time $t = 600$ days. We remark that the major part of the residual contaminant mass in the aquifer is removed. A complete removal of the contaminant is achieved at the final time $t = 875$ days, as illustrated by Figure 10.

Finally, Figure 11 reports the residual contaminant mass in the aquifer as a decreasing function of time and summarizes the performance of the different remediation approaches $T2$, $T3$ and $T4$. This figure emphasizes how the bioremediation strategy can be more effective than the simple pump-and-treat method. Although both intervention strategies $T2$ and $T4$ achieves an almost complete removal of the contaminant, the remediation time is very different in the two cases. Nevertheless, bioremediation can also be sensitive to the well configuration network chosen for the intervention, as shown by the performance curve $T3$.

4.1. Model performance

In this section, we report some information about the simulation costs in terms of computer time.

All the simulations described in the previous section were run on a computational mesh composed of about 5000 triangles using an IBM RISC 6000/390 machine. The simulations involving the full four-species model are very expensive and take about 12 h, while single-species calculations require typically 80–90 min.

The CPU cost is quite high in the former case because all of the non-linear interactions among the different species must be taken into account. These interactions yield a 4×4 non-linear systems which must be solved for each cell at each time step. Using a Newton iterative

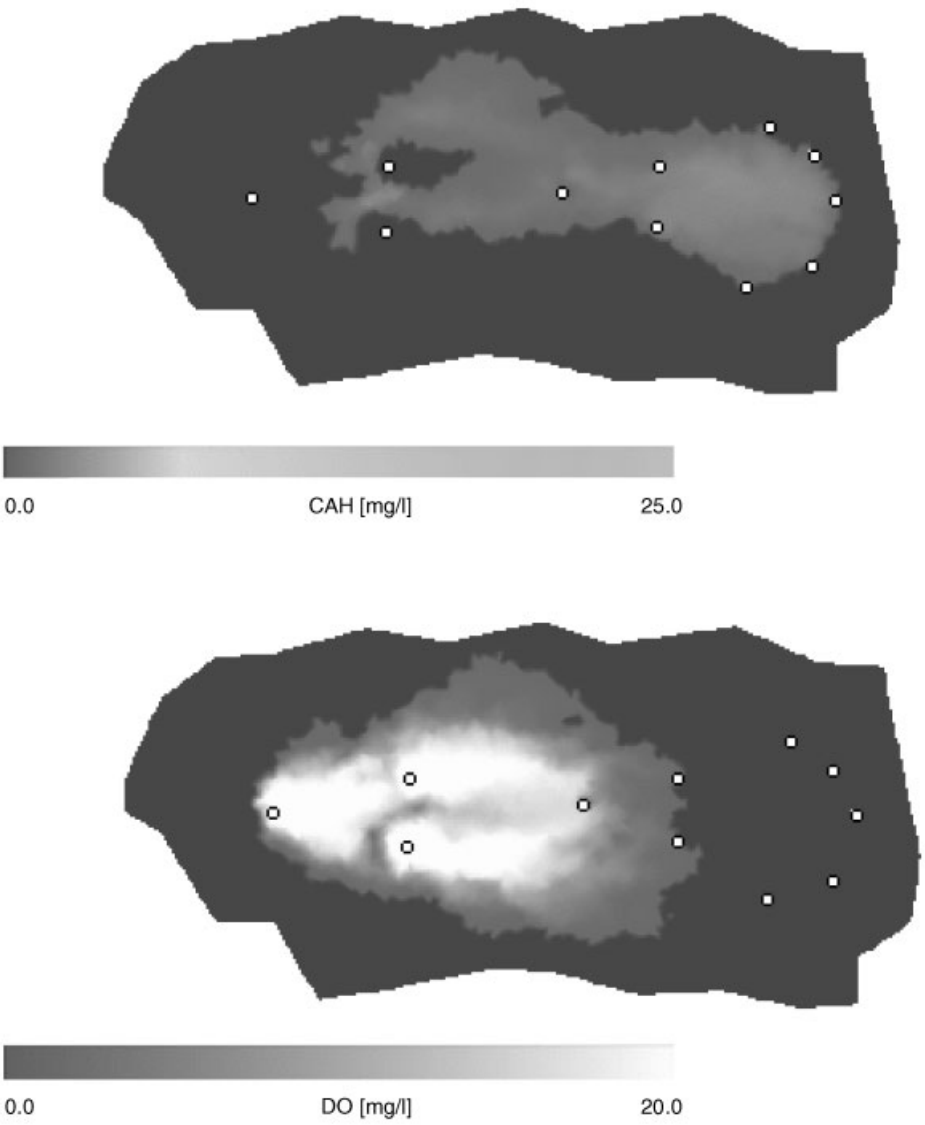

Figure 7. Bioremediation by first well configuration ($T3$): concentration at $t = 178$ days.

scheme this takes approximately 40% of the total CPU costs. Moreover, the finite volume method requires a limited piecewise-linear reconstruction of each unknown field to ensure second-order accuracy in space. The limiting procedure is needed to ensure monotonicity of reconstructed gradients and to preserve non-linear stability [20]. The computational cost of the reconstruction procedure is also significant, being about 35% of the total CPU cost of the

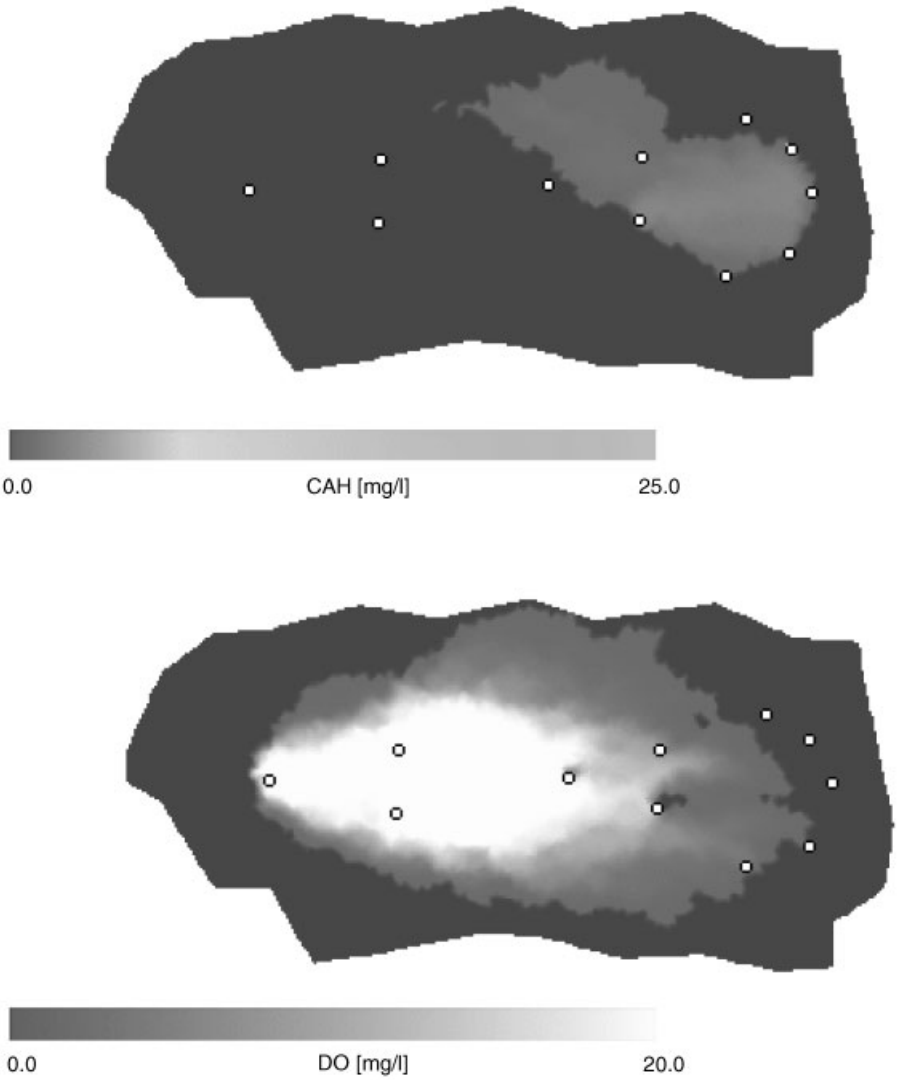

Figure 8. Bioremediation by first well configuration ($T3$): concentration at $t = 360$ days.

simulation. This increment is evident when the full species model is considered instead of the single-species one.

The CPU cost is also influenced by the way the simulation is run. For instance, in the initial contamination phase $T1$, the pollutant is transported by a steady groundwater flow field, which is computed only once at the beginning of the run. Instead, simulation $T2$ still involves a single-species model, but makes usage of a transient groundwater velocity field, which is updated every 50 transport steps, thus resulting in a 10–15% more expensive computation.

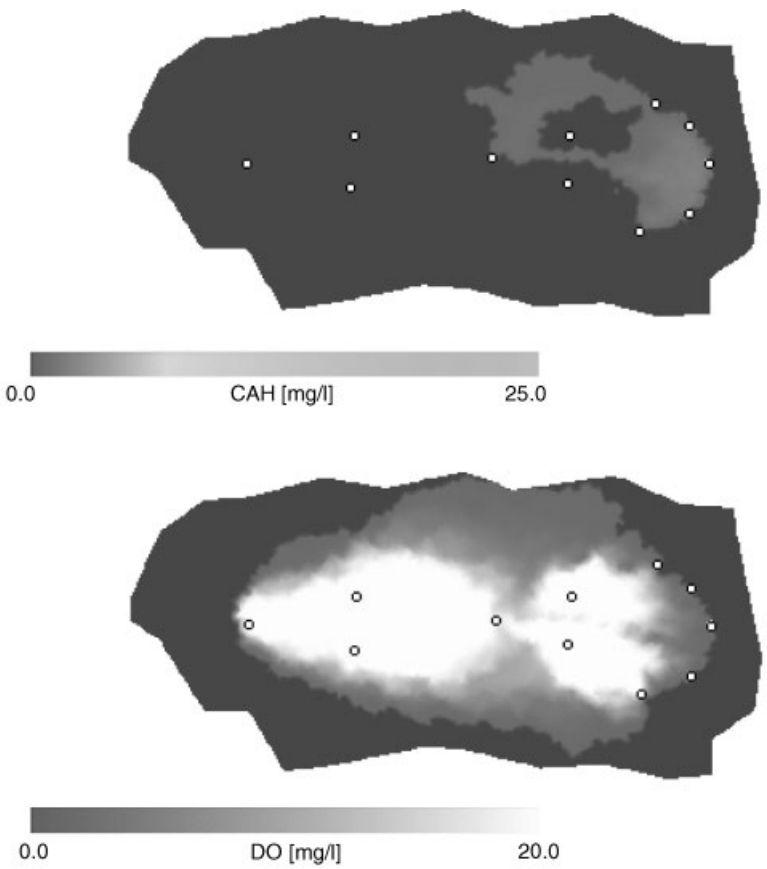

Figure 9. Bioremediation by second well configuration ($T4$): concentration at $t = 600$ days (200 days after the switch).

5. CONCLUSIONS

In this work, we illustrated a numerical model to simulate the bioremediation process in heterogeneous saturated aquifers and its application in devising different intervention strategies on a field-size scenario. The method is particularly suitable in detecting possible dead-zones due to the heterogeneity of the medium and depending on the well location and operational mode.

Our approach is based on the discretization of a multispecies transport model coupled with a bacterial degradation kinetics of Monod type. The microcolony description of bacterial activity is considered. The bulk flow velocity is approximated by a mixed-hybrid finite element method while the species transport equations are discretized using a semi-implicit cell-centre finite volume scheme.

The performance of the method is assessed by simulating both the contamination process and several remediation strategies on a realistic subsurface scenario.

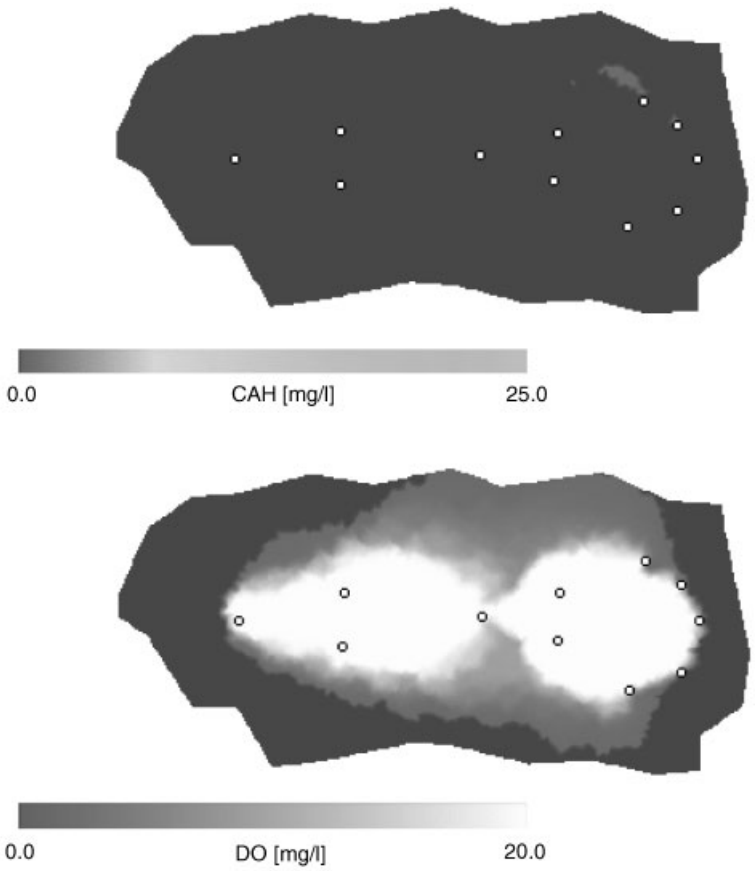

Figure 10. Bioremediation by second well configuration ($T4$): concentration at $t = 875$ days (475 days after the switch).

A comparison between the numerical experiments reported in this work clearly illustrates the advantage of a combined *biological-hydraulic* intervention with respect to the simple *hydraulic* one in the case of a stochastically heterogeneous soil. The remediation time in the former case is shown to be about one-half that of the latter case. This implies that the operational costs may be substantially reduced.

When the aquifer is strongly heterogeneous, preferential flow zones may appear and large spots of contaminant may remain isolated if the simplest pump-and-treat remediation strategy is adopted. Contaminant trapping effects due to heterogeneities may also be present when remediation is enhanced by bacterial activity. In such a case, an optimal well configuration has a dramatic impact on the effectiveness of the human intervention. For these reasons, it is evident that a better understanding of how and where trapping zones may appear is critical in devising an effective remediation strategy.

In order to study the near-source contamination zone, that is the zone surrounding an organic contaminant spill, a multiphase model is needed, given the presence of an immiscible organic phase. It is informative to say that some preliminary work [12, 27] has been performed

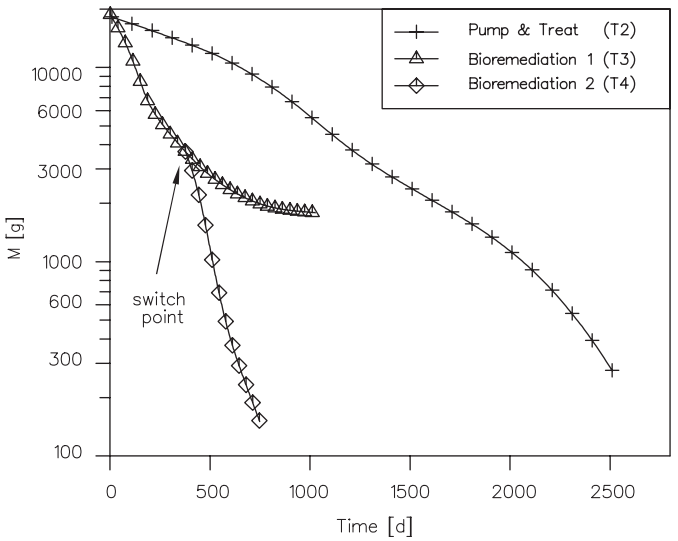

Figure 11. Contaminant residual mass removal vs. remediation time.

by the authors to develop a suitable numerical approach to multiphase simulations as well as considering the problem of pore-clogging in biofilm models. However, these topics will be the issue of future work.

APPENDIX A

The kinetic degradation rates of concentrations within microcolonies in Equation (3) for the four species model used in all of the simulations are

$$\kappa_S A_c \frac{(C_S - c_S)}{\delta} = m_c Y_{S,O} \mu_{0,O} \left[\frac{c_S}{K_{S,O} + c_S}\right] \left[\frac{c_O}{K_O + c_O}\right] \left[\frac{c_A}{K_{A,O} + c_A}\right] + m_c Y_{S,N} \mu_{0,N} \left[\frac{c_S}{K_{S,N} + c_S}\right] \left[\frac{c_N}{K_N + c_N}\right] \left[\frac{c_A}{K_{A,N} + c_A}\right] I_b^1 \tag{A1}$$

$$\kappa_O A_c \frac{(C_O - c_O)}{\delta} = m_c Y_O \mu_{0,O} \left[\frac{c_S}{K_{S,O} + c_S}\right] \left[\frac{c_O}{K_O + c_O}\right] \left[\frac{c_A}{K_{A,O} + c_A}\right] + \alpha_O k_{d,O} \left[\frac{c_O}{K_{O'} + c_O}\right] \tag{A2}$$

$$\kappa_N A_c \frac{(C_N - c_N)}{\delta} = m_c Y_N \mu_{0,N} \left[\frac{c_S}{K_{S,N} + c_S}\right] \left[\frac{c_N}{K_N + c_N}\right] \left[\frac{c_A}{K_{A,N} + c_A}\right] I_b^1 + \alpha_N k_{d,N} \left[\frac{c_N}{K_{N'} + c_N}\right] I_b^1 \tag{A3}$$

$$\kappa_A A_c \frac{(C_A - c_A)}{\delta} = m_c Y_{A,O} \mu_{0,O} \left[\frac{c_S}{K_{S,O} + c_S}\right] \left[\frac{c_O}{K_O + c_O}\right] \left[\frac{c_A}{K_{A,O} + c_A}\right] + m_c Y_{A,N} \mu_{0,N} \left[\frac{c_S}{K_{S,N} + c_S}\right] \left[\frac{c_N}{K_N + c_N}\right] \left[\frac{c_A}{K_{A,N} + c_A}\right] I_b^1 \quad \text{(A4)}$$

and the microbial growth/decay equation is

$$\frac{1}{N_c} \frac{\partial \phi N_c}{\partial t} = \left(\mu_{0,O} \left[\frac{c_S}{K_{S,O} + c_S}\right] \left[\frac{c_O}{K_O + c_O}\right] \left[\frac{c_A}{K_{A,O} + c_A}\right] - k_{d,O}\right) + \left(\mu_{0,N} \left[\frac{c_S}{K_{S,N} + c_S}\right] \left[\frac{c_N}{K_N + c_N}\right] \left[\frac{c_A}{K_{A,N} + c_A}\right] - k_{d,N}\right) I_b^1 \quad \text{(A5)}$$

where

— $\kappa_S = 1.03 \times 10^{-5}$ (m^2/day), $\kappa_O = 2.19 \times 10^{-5}$ (m^2/day), $\kappa_N = 1.50 \times 10^{-5}$ (m^2/day), $\kappa_A = 1.86 \times 10^{-5}$ (m^2/day) are the mass exchange coefficients for the bulk flow and the microcolony species concentrations;
— $A_c = 3.768 \times 10^{-10}$ (m^2), is the contact area of the microcolony for the mass diffusion process;
— $\delta = 5.0 \times 10^{-4}$ (m) is the thickness of the boundary layer between bulk flow and microcolonies;
— $m_c = 2.86 \times 10^{-11}$(kg) is the microcolony mass;
— $\mu_{0,O} = 4.34$ (1/day) and $\mu_{0,N} = 2.9$ (1/day) are the specific aerobic and anaerobic growth rates;
— $Y_{S,O} = 0.278$ and $Y_{S,N} = 0.5$ are the heterotrophic yield coefficients;
— $Y_O = 0.278$ (–) and $Y_N = 0.5$ (–) are the coefficients for the oxygen and nitrogen synthesis of heterotrophic biomass;
— $\alpha_0 = 0.0402$ (–) and $\alpha_N = 0.1$ (–) are the oxygen and nitrogen use-coefficients for maintenance energy of bacteria;
— $Y_{A,O} = 0.122$ and $Y_{A,N} = 0.122$ are the ammonia–nitrogen coefficients for producing biomass under aerobic and anaerobic conditions;
— $K_{S,O} = 40$ (g/m^3), $K_O = 0.77$ (g/m^3), and $K_{A,O} = 1$ (g/m^3) are the substrate, oxygen, and ammonia–nitrogen saturation constants under aerobic conditions;
— $K_{S,N} = 40$ (g/m^3), $K_N = 2.6$ (g/m^3), and $K_{A,N} = 1$ (g/m^3) are the substrate, nitrogen, and ammonia–nitrogen saturation constants under anaerobic conditions;
— $K_{O'} = 0.77$ (g/m^3) and $K_{N'} = 2.6$ (g/m^3) are the oxygen and nitrogen saturation constants;
— $I_b^0 = 1$ and $I_b^1 = K_{b,N}/(K_{b,N} + c_O)$ are the inhibition functions of the oxygen-based and the nitrogen-based respiration, and $K_{b,N} = 0.0001$ (g/m^3) is the inhibition coefficient;
— $k_{d,O} = 0.02$ (1/day) and $k_{d,N} = 0.02$ (1/day) are the bacterial death-per-unit-time decay constants for aerobic and anaerobic metabolism.

ACKNOWLEDGEMENTS

The work of Claudio Gallo has been financially supported by Sardinian Regional Authorities. The authors would like to thank Dr. Fabio Bettio (CRS4) for his help in visualization and Dr. Enrico Bertolazzi (University of Trento, Italy) for his careful reading of the preliminary version of the paper and his useful suggestions. The unstructured Delaunay grids used in all these simulations were generated by the mesh generator TRIANGLE, a code implemented by Shewchuck, see the *URL*: `http://almond.srv.cs.cmu.edu/afs/cs/project/quake/public/www/triangle.html`.

REFERENCES

1. Davis EL. How heat can enhance in-situ and aquifer remediation: important chemical properties and guidance on choosing the appropriate technique. *Technical Report EPA/540/S-97/502*, US EPA, Technology Innovation Office, Office of Solid Waste and Emergency Response, US EPA, Washington, DC, 1997.
2. Environmental Protection Agency. State policies concerning the use of injectants for *in situ* ground water remediation. *Technical Report EPA/542/S-96/001*, US EPA, Technology Innovation Office, 1996.
3. McCaulou DR, Jewett DG, Huling SG. Non-aqueous phase liquids compatibility with materials used in well construction, sampling, and remediation. *Technical Report EPA/540/S-95/503*, US EPA, Technology Innovation Office, Office of Solid Waste and Emergency Response, US EPA, Washington, DC, 1995.
4. National Research Council. *In-Situ Bioremediation*: *When Does it Work*? National Academy Press: Washington, DC, 1993.
5. Ross RR. General methods for remedial operations performance evaluations. *Technical Report EPA/600/R-92/002*, US EPA, Technology Innovation Office, Office of Solid Waste and Emergency Response, US EPA, Washington, DC, 1992.
6. Russel HH, Matthews JE, Sewell GW. TCE removal from contaminated soil and groundwater. *Technical Report EPA/540/S-92/002*, US EPA, Technology Innovation Office, Office of Solid Waste and Emergency Response, US EPA, Washington, DC, 1992.
7. Bear J. *Hydraulics of Groundwater*. McGraw-Hill: New York, 1979.
8. Kelly WR, Hornberger GM, Herman JS, Mills AL. Kinetics of BTX biodegradation and mineralization in batch and column systems. *Journal of Contamination Hydrology* 1996; **23**:113–132.
9. Lensing JJ, Vogt M, Herrling B. Modelling biologically mediated redox processes in the subsurface. *Journal of Hydrology* 1994; **159**:125–143.
10. Bailey JE, Ollis DF. *Biochemical Engineering Fundamentals*. McGraw-Hill: New York, 1977.
11. National Research Council. *Alternatives for Ground-water Cleanup*. National Academy Press: Washington, DC, 1994.
12. Gallo C, Hassanizadeh SM. Influence of biodegradation on NAPL flow and dissolution in groundwater. In *Computational Methods in Water Resources XIII*, Bentley LR *et al.* (eds), vol. 1. A. A. Balkema: Rotterdam, Holland, 2000; 129–136.
13. Hassanizadeh SM. Upscaling equations of solute transport and biodegradation in soils. *Technical Report*, Department of Civil Engineering and Geosciences, TUDelft, The Netherlands, 1999.
14. Kindred JS, Celia MA. Contaminant transport and biodegradation: 2. Conceptual model and test simulations. *Water Resources Research* 1989; **25**(6):1149–1159.
15. Molz FJ, Widdowson MA, Benefield LD. Simulation of microbial growth dynamics coupled to nutrient and oxygen transport in porous media. *Water Resources Research* 1986; **22**(8):1207–1216.
16. Taylor SW, Jaffè PR. Substrate and biomass transport in a porous medium. *Water Resources Research* 1990; **26**(9):2181–2194.
17. Baveye P, Valocchi A. An evaluation of mathematical models of the transport biologically reacting solutes in saturated soils and aquifers. *Water Resources Research* 1989; **25**(6):1413–1421.
18. Widdowson MA, Molz FJ, Benefield LD. A numerical transport model for oxygen- and nitrate-based respiration linked to substrate and nutrient availability in porous media. *Water Resources Research* 1988; **24**(9): 1553–1565.
19. Bergamaschi L, Gallo C, Manzini G, Paniconi C, Putti M. A mixed finite-elements/TVD finite-volumes scheme for saturated flow and transport in groundwater. In *Finite Elements in Fluids*, Cecchi *et al.* (eds). Padova: Italy, 1995; 1223–1232.
20. Gallo C, Manzini G. A mixed finite element/finite volume approach for solving biodegradation transport in groundwater. *International Journal for Numerical Methods in Fluids* 1998; **26**:533–556.
21. Gallo C, Manzini G. 2-D numerical modelling of bioremediation in heterogeneous saturated soils. *Transport in Porous Media* 1998; **31**:67–88.
22. Gallo C, Manzini G. Finite volume/mixed finite element analysis of pollutant transport and bioremediation in heterogeneous saturated aquifers. *Technical Report 1200*, IAN, 2001.

23. Freeze RA, Cherry JA. *Groundwater*. Prentice-Hall: Englewood Cliff, NJ, 1979.
24. Ciarlet PG. *The Finite Element Method for Elliptic Problems*. North-Holland: Amsterdam, Holland, 1980.
25. Brezzi F, Fortin M. *Mixed and Hybrid Finite Element Methods*. Springer: Berlin, 1991.
26. Chavent G, Roberts JE. A unified physical presentation of mixed, mixed-hybrid finite elements and standard finite difference approximation for the determination of velocities in waterflow problems. *Advances in Water Resources* 1991; **14**(6):329–348.
27. Gallo C, Manzini G. A fully coupled numerical model for two-phase flow with contaminant transport and biodegradation kinetics. *Communications in Numerical Methods in Engineering* 2001; **17**:325–336.

